

Supplemental Materials

Arthur Omran^{1,2,*}, Asbell Gonzalez ¹, Cesar Menor-Salvan ³, Michael Gaylor ⁴,
Jing Wang ⁵, Jerzy Leszczynski ⁵ and Tian Feng ²

1 Department of Chemistry, University of North Florida, Jacksonville, FL 32224, USA

2 Department of Geosciences, University of South Florida, Tampa, FL 33620, USA

3 Departamento de Biología de Sistemas, Universidad de Alcalá, 28805 Alcalá de Henares, Spain

4 Analytical Sciences, Small Molecules Technologies, Bayer U.S., Saint Louis, MO 63167, USA

5 Department of Chemistry, Physics and Atmospheric Sciences, Jackson State University, Jackson, MS 39217, USA

* Correspondence: arthur.omran@unf.edu

Table of Contents	Page Number
1 Additional Methods	3
2 Additional Results	4
Figure S1 Raman Spectrum of Ca/Mg chemical garden	4
Figure S2 Raman Spectrum of olivine sample	4
Figure S3 Raman Spectrum of serpentinite	5
Figure S4 Powder XRD diffraction pattern for olivine	5
Figure S5 Powder XRD diffraction pattern for serpentine	6
Figure S6 Hydrothermal alteration of the chemical garden	7
Figure S7 Concentrated formose reaction proton NMR	8
Figure S8 C13 NMR of a Ca/Mg-Based chemical garden facilitated formose reaction	9
Figure S9 Formose solution with no spiked in products.	10
Figure S10 Spiked in-experiment.	10
Figure S11 Spiked in-experiment. Overlay	11
Figure S12 HSQC of C ¹³ (y axis) with H ¹ NMR (x axis) of a formose sample	11
	1

Table S1 Detected sugar values. Mass and Mol % of the glycosyl residues	12
Figure S13 Gas Chromatogram for the control formose reaction	12
Figure S14 Gas Chromatogram for the formose reaction with Ca/Mg chemical gardens	13
Figure S15 Gas Chromatogram for the formose reaction which contained olivine minerals	13
Figure S16 Gas Chromatogram for the formose reaction which contained serpentinite minerals.	14
Figure S17 Gas Chromatogram for the formose reaction which contained magnetite minerals.	14
Figure S18 Observed reaction times for formose reactions in the presence of different minerals	15
Table S2 Product distributions in formose reactions after 25 minutes.	15
Figure S19 CaCl ₂ MgCl ₂ (all aqueous) formose catalyzed solution proton NMR.	16
Reaction Scheme S1: A model for a protometabolic system on dry land	16
Reaction Scheme S2: A model for a protometabolic system at a hydrothermal vent	17
Figure S20 Sugar break down control. 0.167 Glucose solution heated at 90 C for 30 minutes at pH. 12.5 proton NMR. We see the same peaks for lactic acid as we do in our formose reactions	17

1 Additional Methods

GCMS of Formose Samples to Detect Trace Sugar Species

Glycosyl composition analysis was performed by combined gas chromatography/mass spectrometry (GC/MS). Per-O-trimethylsilyl (TMS) derivatives of monosaccharide methyl glycosides were produced from the sample by acidic methanolysis. The dried formose sample (1.8 mg) with inositol (internal standard, 20 µg) was heated with methanolic HCl for 18 h at 80 °C. After cooling to room temperature and removal of the solvent under a stream of nitrogen, the samples were treated with a mixture of methanol, pyridine, and acetic anhydride for 30 minutes. The solvents were evaporated in a fume hood overnight. The samples were derivatized with Tri-Sil (Pierce) at 80 °C for 30 min. GC/MS analysis of the TMS methyl glycosides is performed on an Agilent 7890A GC, using a Supelco Equity-1 fused silica capillary column (30 m × 0.25 mm ID). The mixture of derivatized sample was analyzed by GC-MS and per-O-trimethylsilyl derivatives of monosaccharide residues run alongside the sample and used for quantification of each monosaccharide residue. The peak integration was used for quantification.

2 Additional Results

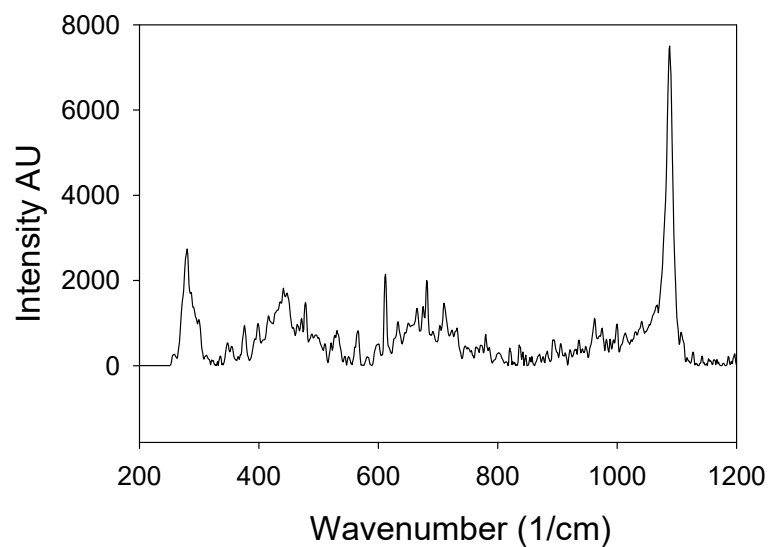


Figure S1. Raman Spectrum of Ca/Mg chemical garden. Spectrum taken with a 780 nm laser. Verified against RRUFF mineral database.

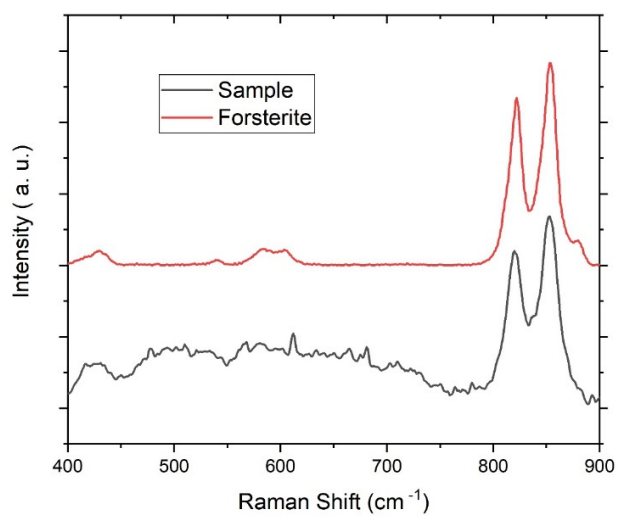


Figure S2. Raman Spectrum of olivine sample. Spectrum taken with a 780 nm laser. Verified against RRUFF mineral database.

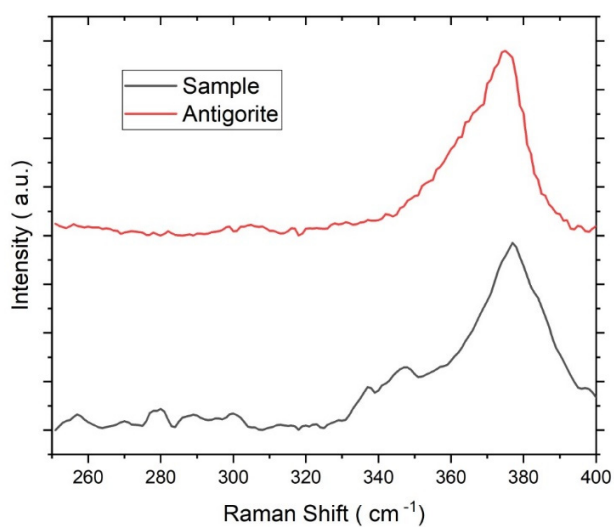


Figure S3. Raman spectrum of serpentinite. Spectrum taken with a 780 nm laser. Verified against RRUFF mineral database.

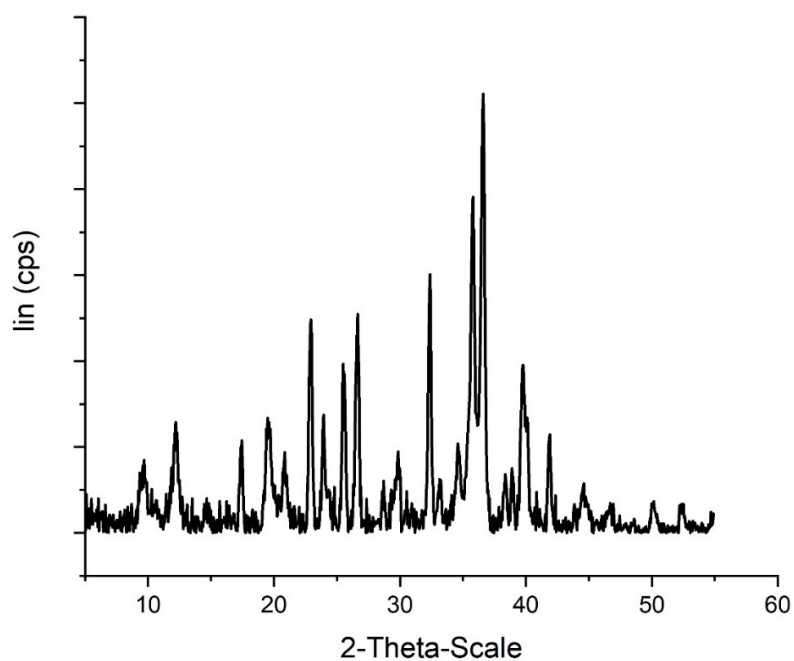


Figure S4. Powder XRD diffraction pattern for olivine. 5 – 55-degree angle used. Verified against RRUFF mineral database.

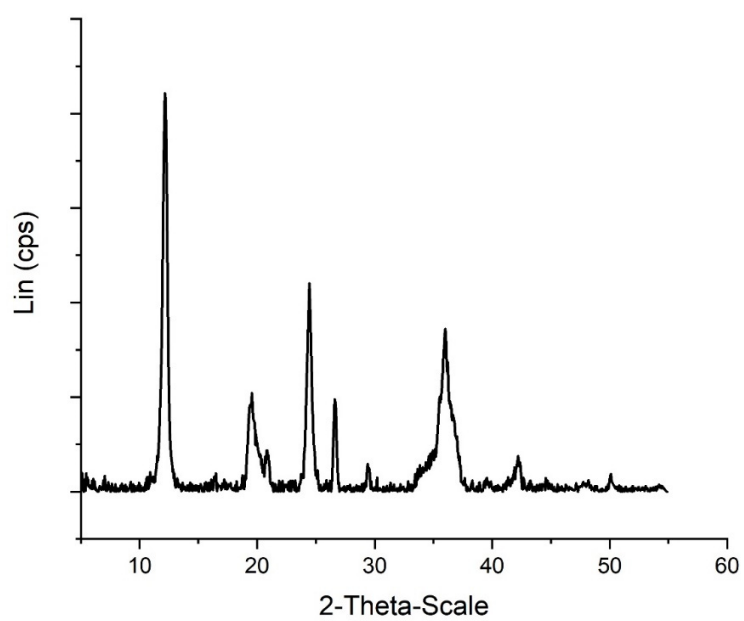


Figure S5. Powder XRD diffraction pattern for serpentine. 5 – 55-degree angle used. Verified against RRUFF mineral database.

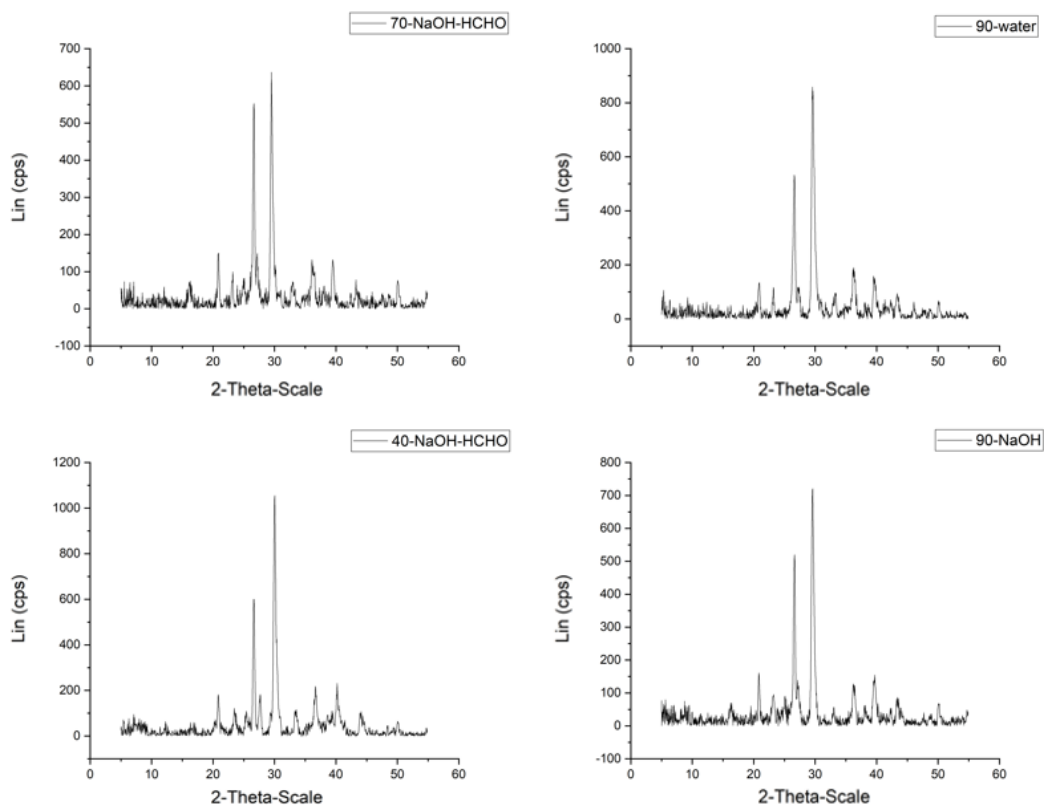


Figure S6. Hydrothermal alteration of the chemical garden. Hydrothermal alteration of the chemical garden occurs during the heating of the water for the formose process. During this process, the chemical garden transitions from a composition of calcite, magnesite, aragonite, brucite, and dolomite to a composition of mostly calcite, with some aragonite and Mg left.

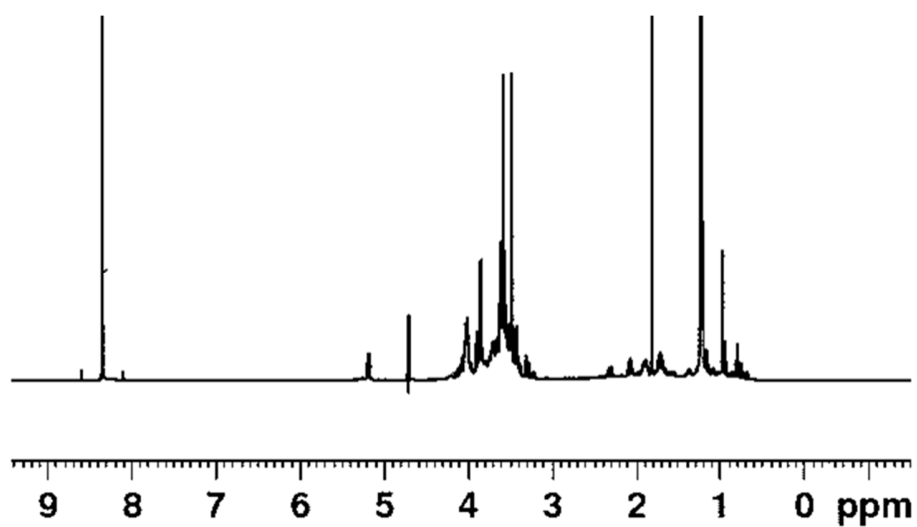


Figure S7. Concentrated Formose reaction. Chemical Garden facilitated reaction, dried overnight in the fume hood. Proton NMR with customized water suppression (noesygprr1d) technique on the Bruker Neo 600 with D₂O Salt Locking. No peak at 3.2 ppm for methanol due to evaporative process.

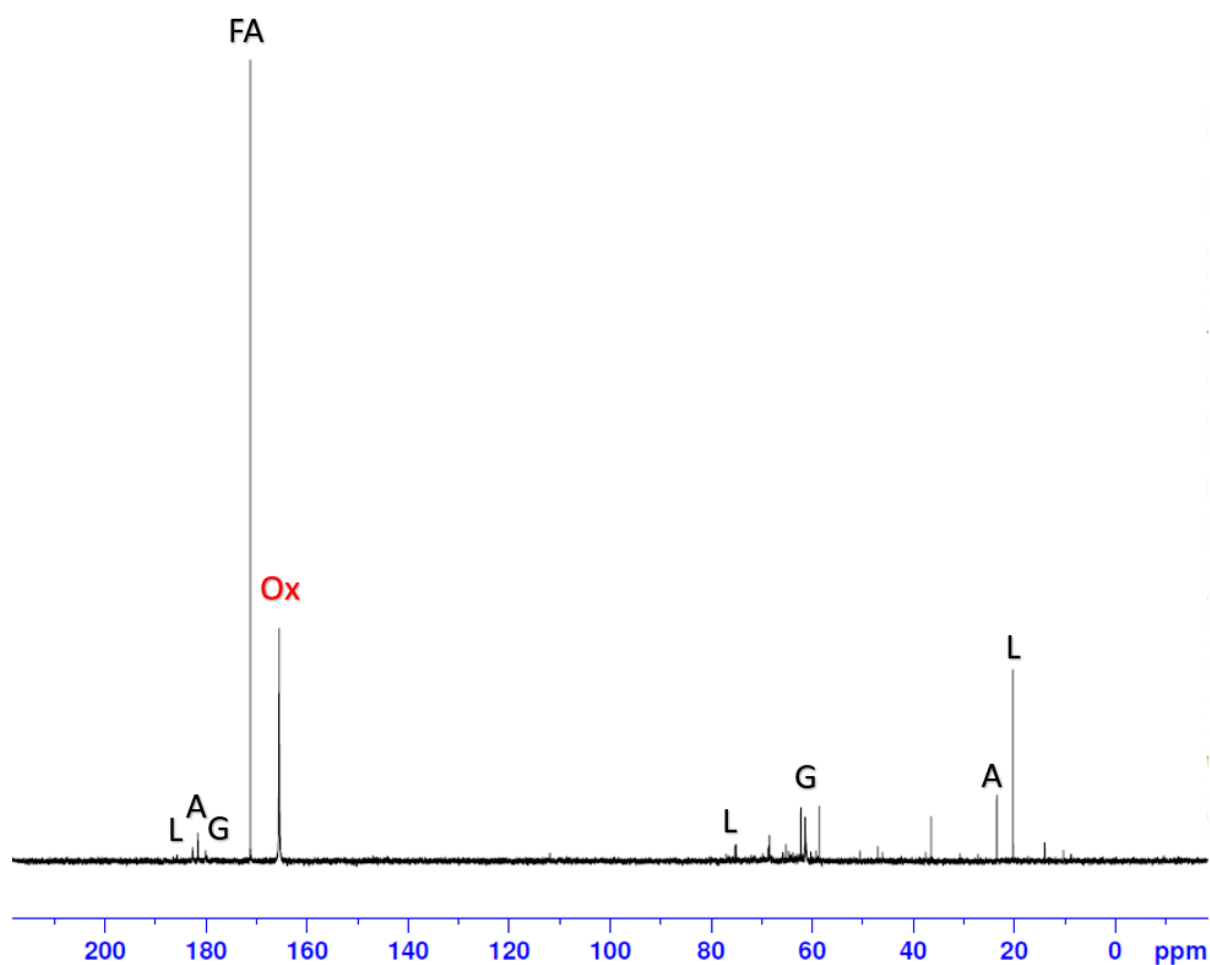


Figure S8. ^{13}C NMR of a Ca/Mg-Based chemical garden facilitated formose reaction. Spectrum shows detection of glycolic acid, G, acetic acid, A, and lactic acid, L. Spectrum also indicates the presence of oxalic acid, Ox, which has yet to be detected in such studies due to it being proton silent.

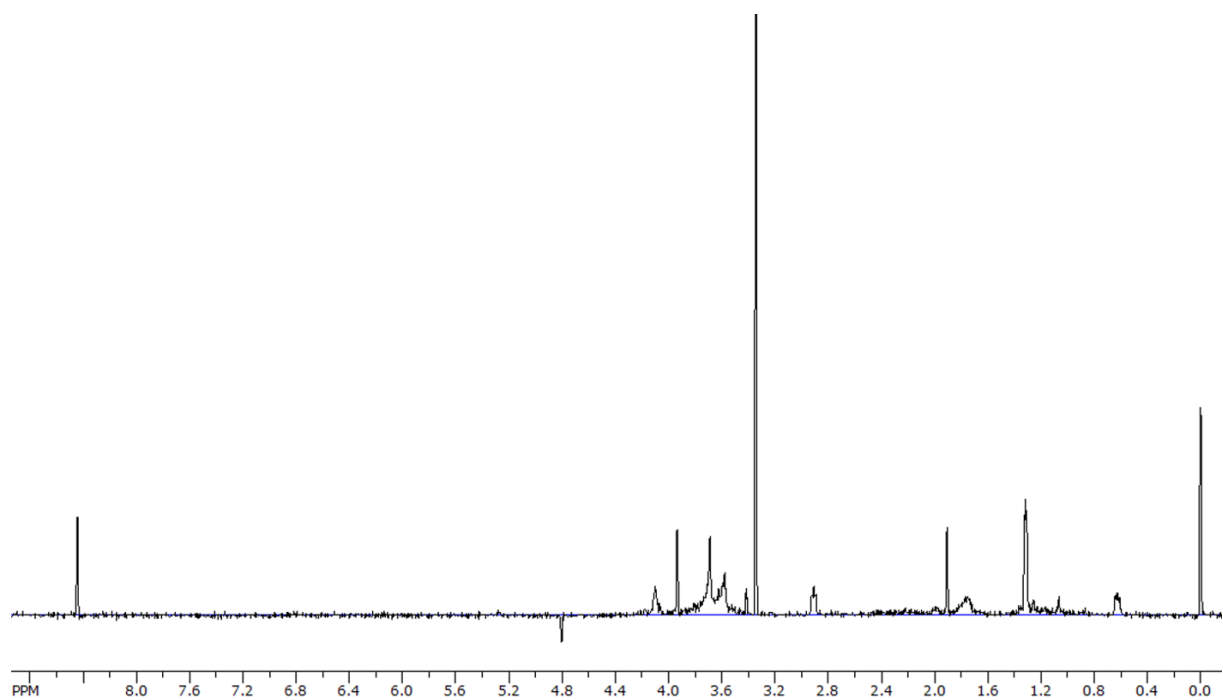


Figure S9. Formose solution with no spiked in products.

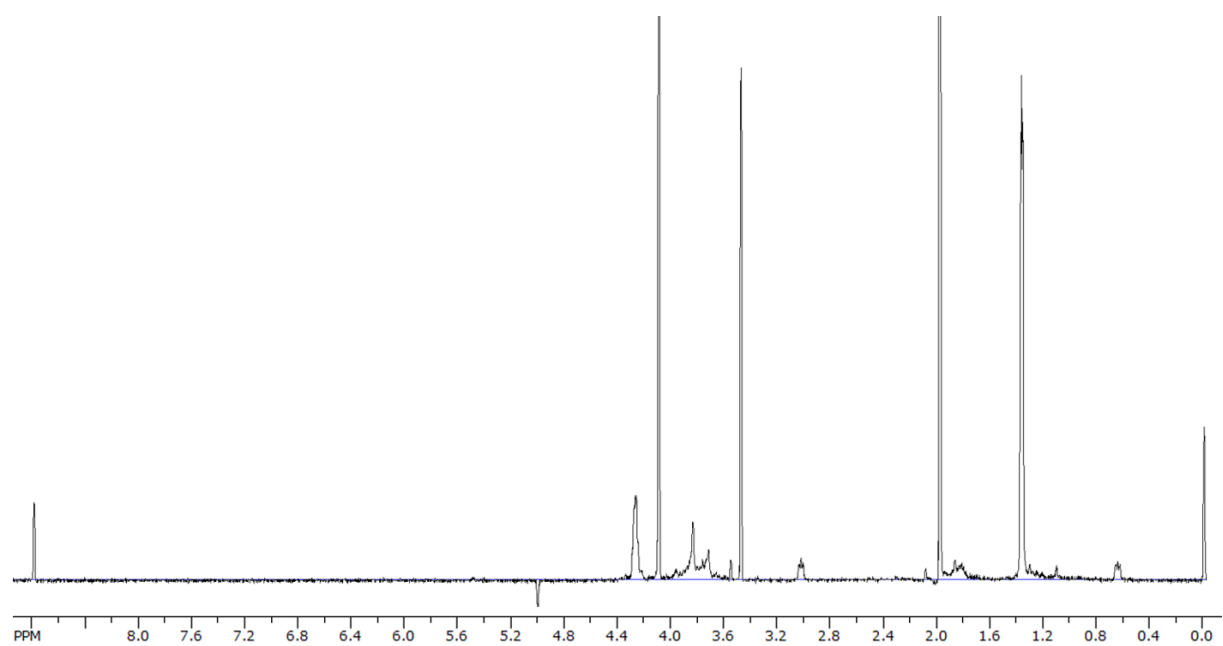


Figure S10. Spiked in-experiment. Formose solution was spiked with glycolic acid, G, acetic acid, A, and lactic acid, L.

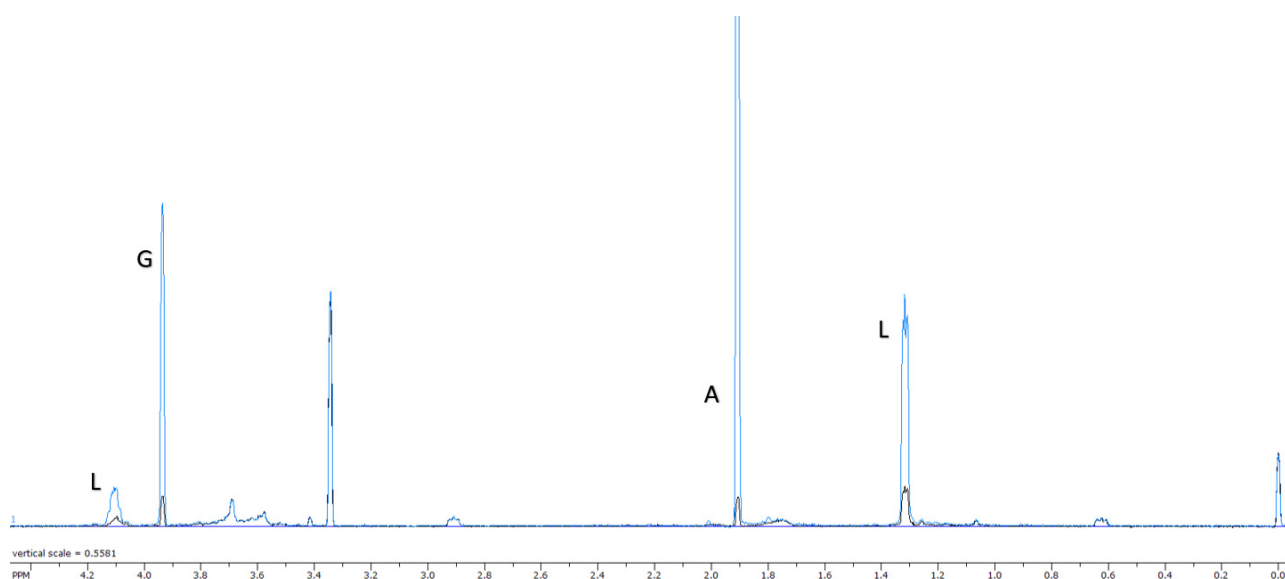


Figure S11. Spiked in-experiment. Formose solution was spiked with glycolic acid, G, acetic acid, A, and lactic acid, L (the blue spectrum). This is overlaid onto a spectrum with no spiked in products (the black baseline spectrum). Spectrum shows clear detection of glycolic acid, G, acetic acid, A, and lactic acid, L. Spectral range from 0 to 4.3 ppm.

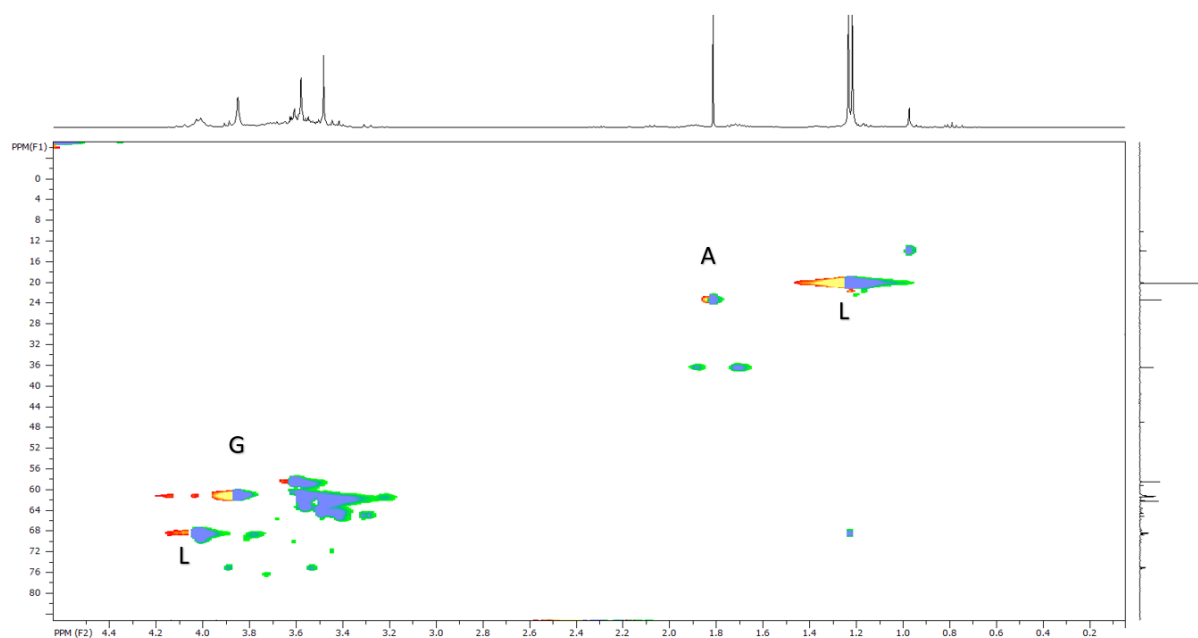


Figure S12. HSQC of C^{13} (y axis) with H^1 NMR (x axis) of a formose sample. Spectrum shows clear detection of glycolic acid, G, acetic acid, A, and lactic acid, L.

Table S1. Detected sugar values. Mass and Mol % of the glycosyl residues identified for the formose reaction dried samples.

	Samples									
	C-Sugar		Garden-Sugar		OP-Sugar		SERP-Sugar		Mag-Sugar	
Glycosyl Residues	Mass (μg)	Mol % ¹	Mass (μg)	Mol % ¹	Mass (μg)	Mol % ¹	Mass (μg)	Mol % ¹	Mass (μg)	Mol % ¹
Arabinose (Ara)	N.D.	-	2.81	15.0	N.D.	-	N.D.	-	N.D.	-
Xylose (Xyl)	Trace	27.0	9.22	49.2	Trace	37.0	Trace	22.6	Trace	53.6
Mannose (Man)	Trace	9.76	1.44	6.40	Trace	1.0	N.D.	-	N.D.	-
Glucose (Glc)	Trace	63.2	6.61	29.4	Trace	62.0	Trace	77.4	Trace	46.4
SUM ¹	Trace	100	20.1	100	Trace	100	Trace	100	Trace	100
Total Carbohydrate % by Weight	Trace	%	1.00	%	Trace	%	Trace	%	Trace	%
Mass of Sample	2 mg		2 mg		2 mg		2 mg		4 mg	

¹Values are expressed as mole percent of total carbohydrate. The total Mol % may not add to exactly 100% due to rounding.

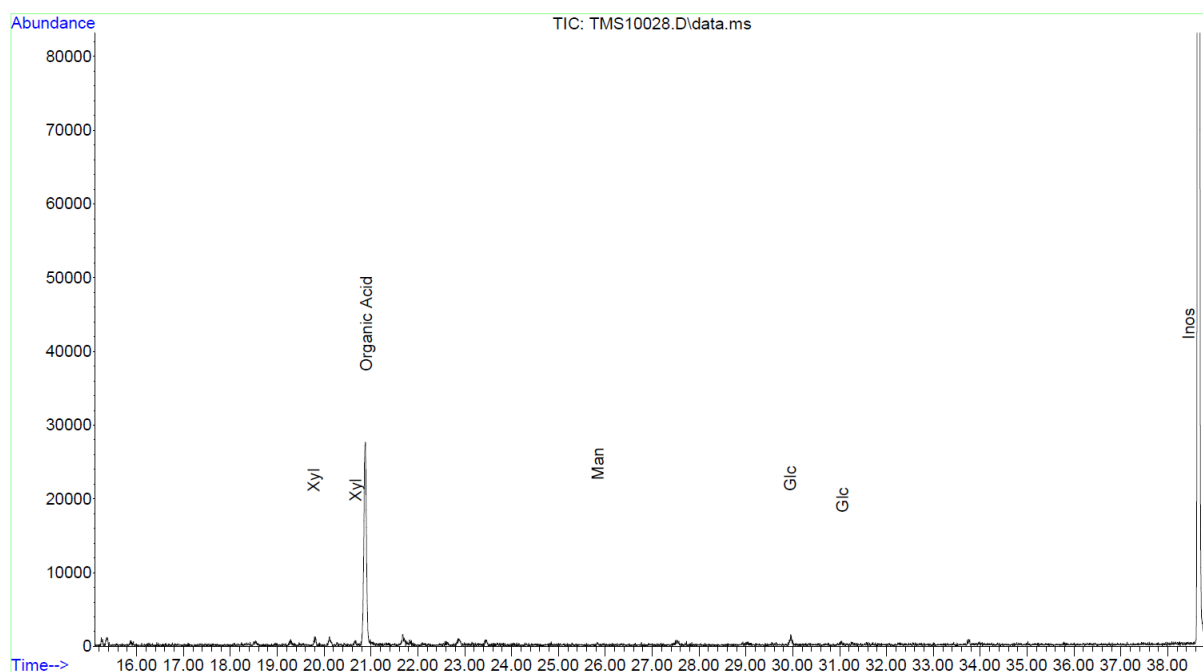


Figure S13. Gas Chromatogram for the control formose reaction which contained no minerals or chemical gardens.

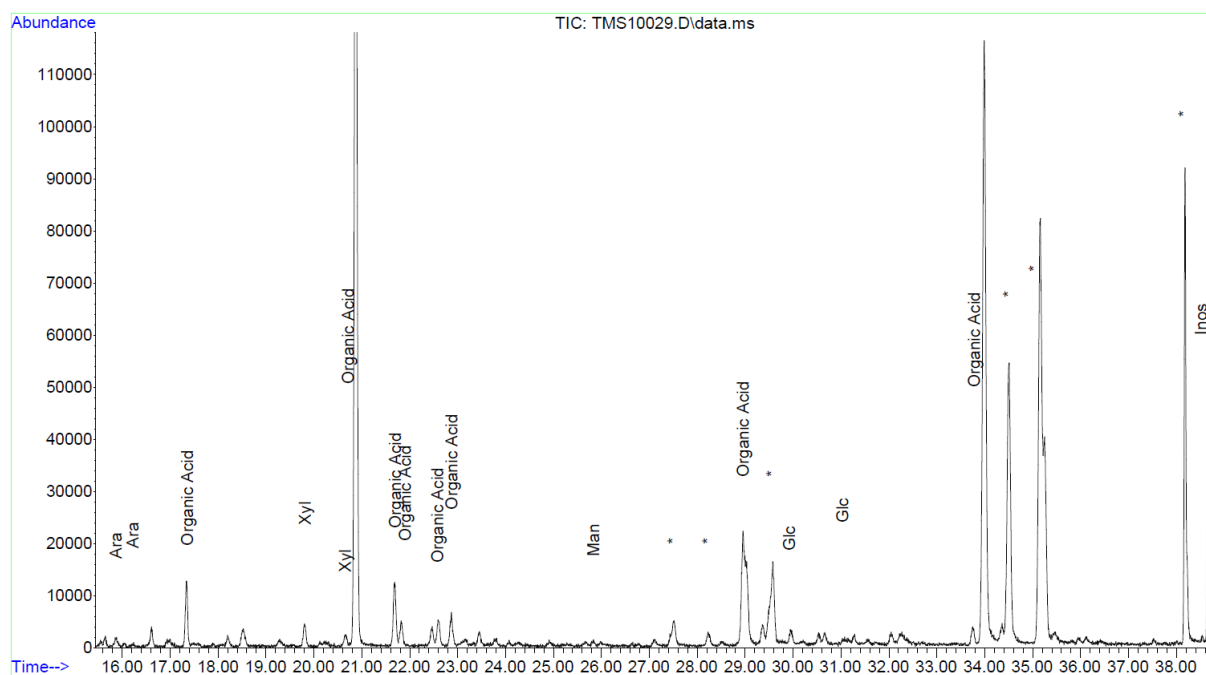


Figure S14. Gas Chromatogram for the formose reaction which contained fragments of Ca/Mg-based chemical gardens. * Represent sugar like signatures that may be branched chain sugar species.

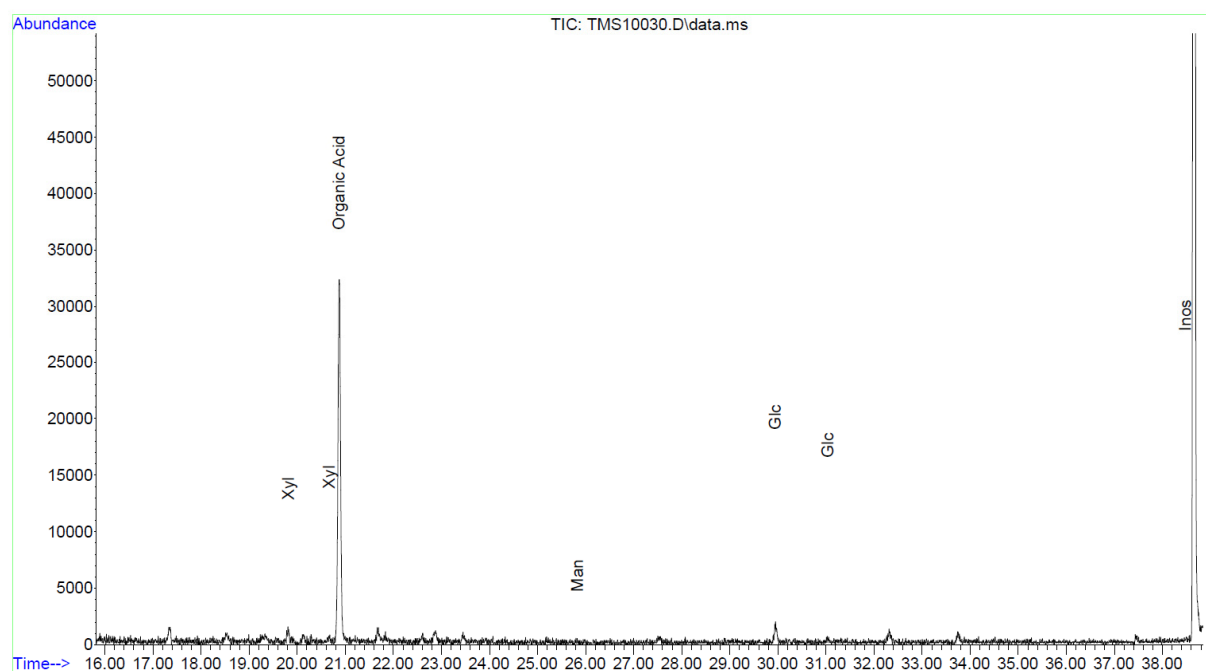


Figure S15. Gas Chromatogram for the formose reaction which contained serpentinite minerals.

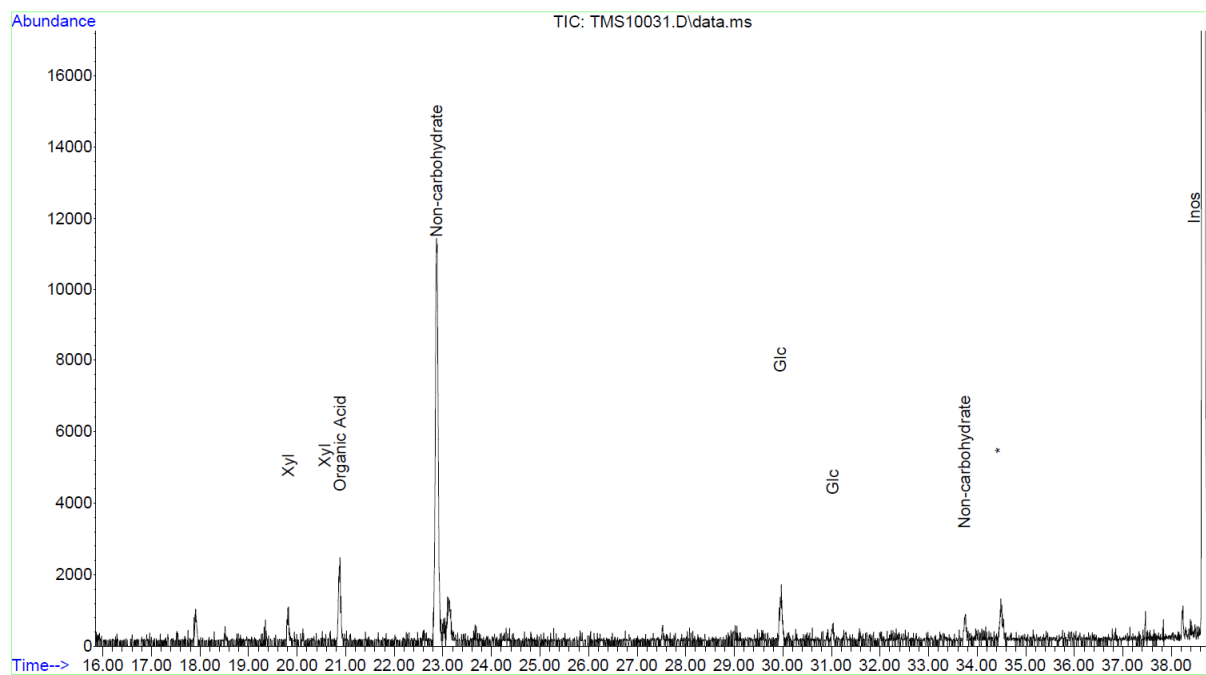


Figure S16. Gas Chromatogram for the formose reaction which contained olivine minerals.

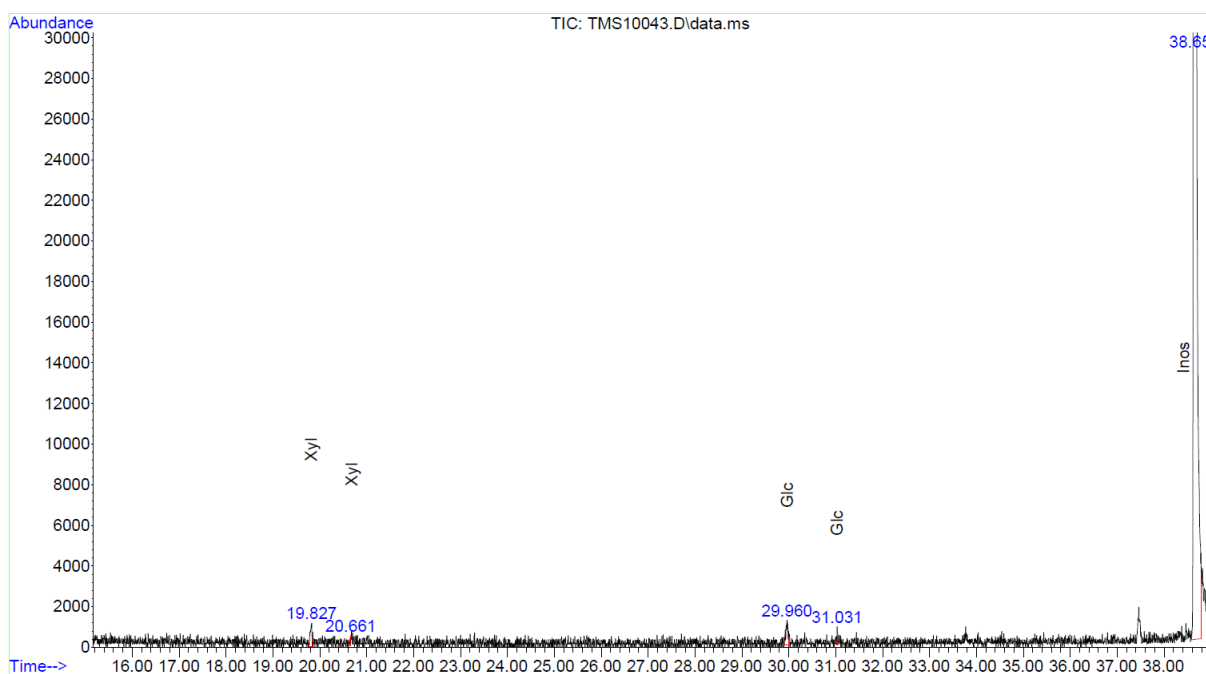


Figure S17. Gas Chromatogram for the formose reaction which contained magnetite minerals.

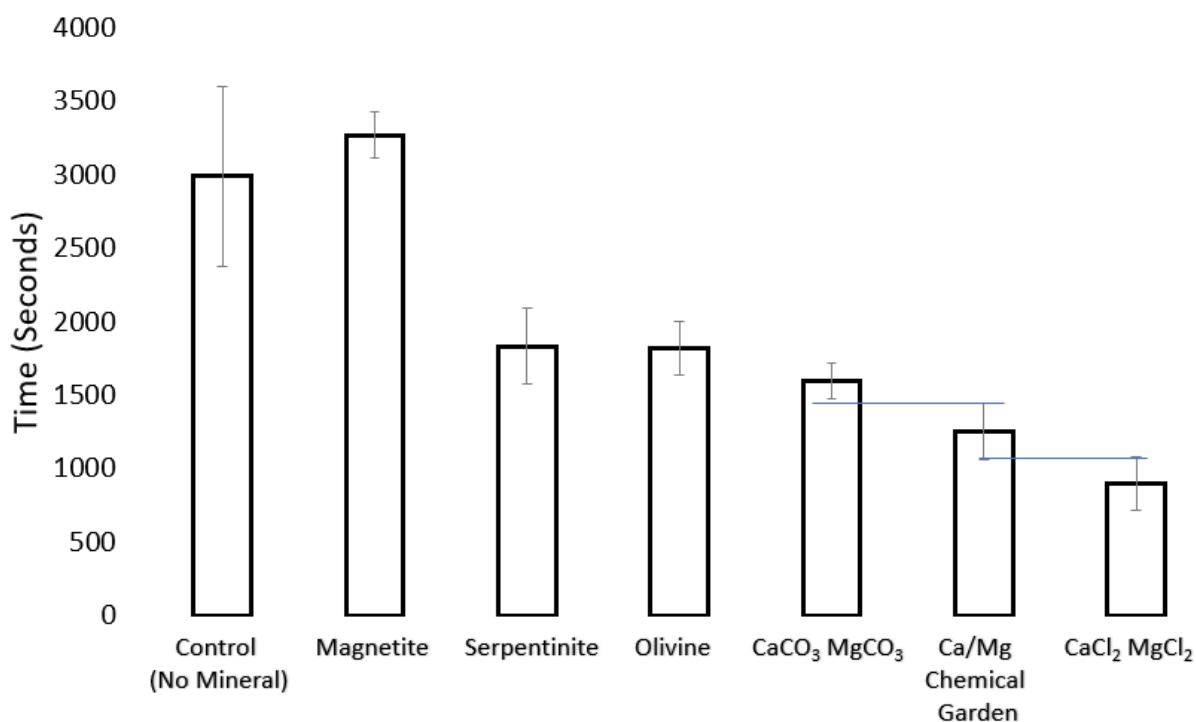


Figure S18. Observed reaction times for formose reactions in the presence of different minerals. The time it took each reaction to yellow, n=3. The chemical garden group was statistically insignificant from the soluble Ca/MgCl₂ group.

Table S2. Product distributions in formose reactions after 25 minutes. Data are from integral percentages.

	Formic Acid	Glycolic Acid	Lactic Acid	Acetic Acid	Methanol	Adsorbed to Mineral
Ca/Mg Chemical Garden	0.12	0.19	0.54	0.15	0.12	0.02
CaCl ₂ MgCl ₂	0.15	0.06	0.52	0.09	0.15	*
CaCO ₃ MgCO ₃	0.2	0.08	0.22	0.09	0.2	0.41
Serpentinite	0.24	0.07	0.36	0.08	0.24	0.01
Olivine	0.2	0.08	0.31	0.07	0.2	0.14
Magnetite	0.22	0	0	0	0.22	0.56
No Mineral	0.26	0	0	0	0.26	*

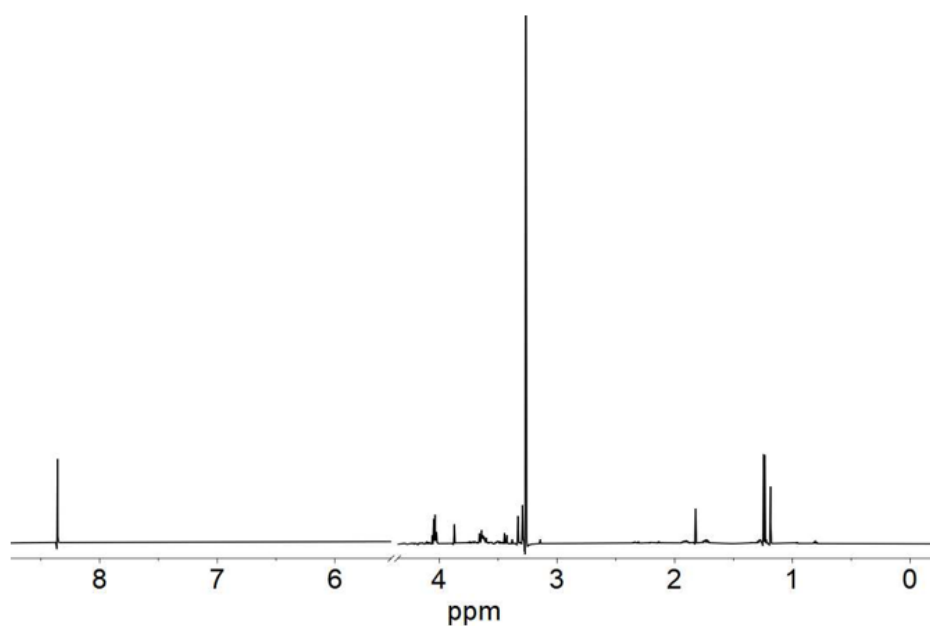
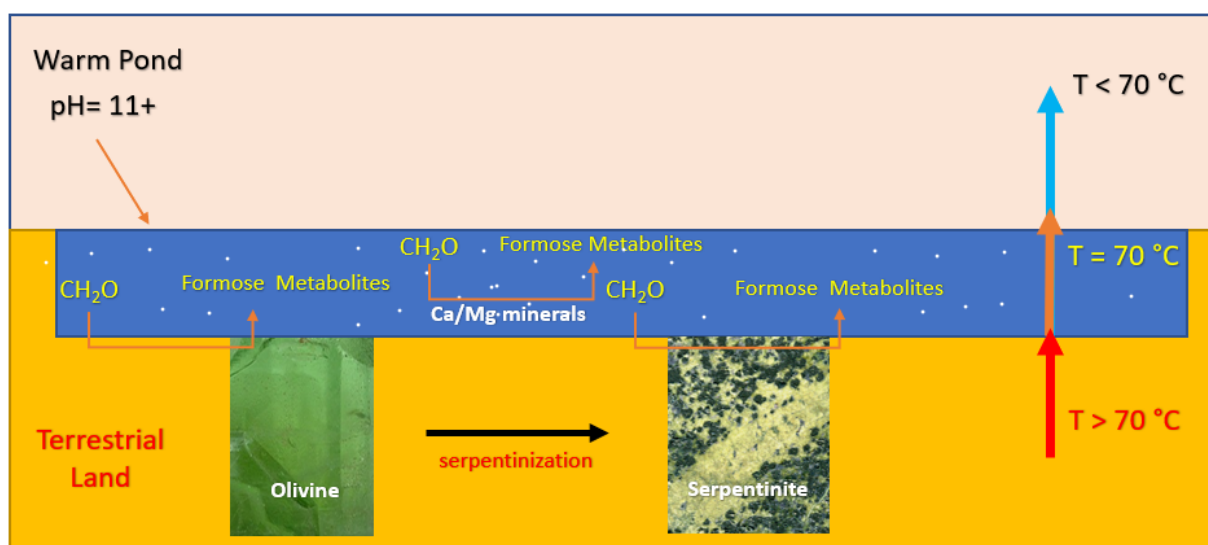
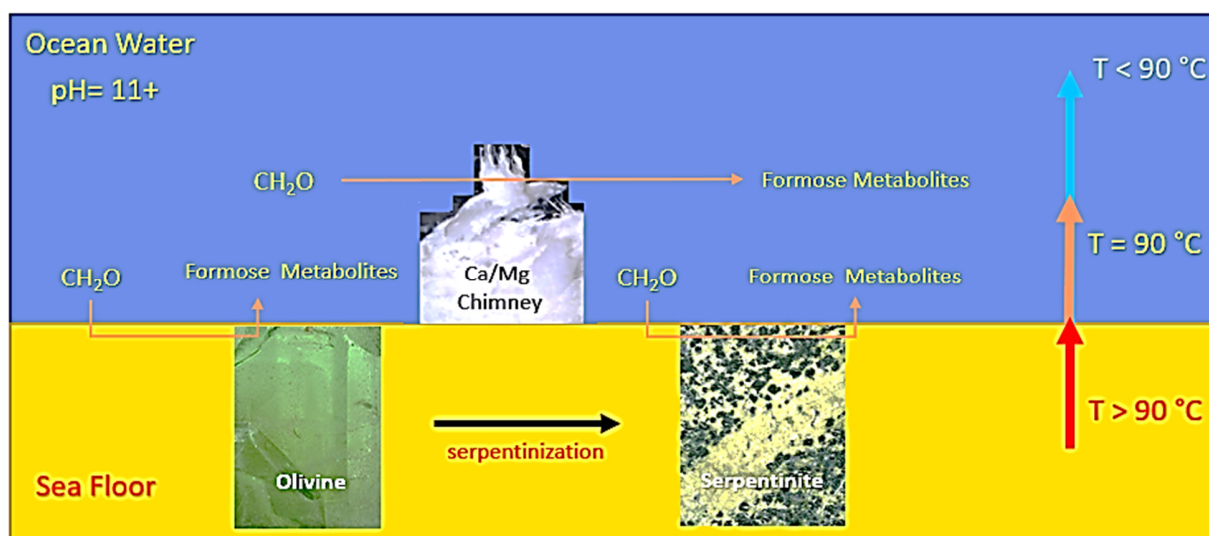


Figure S19. CaCl_2 MgCl_2 (all aqueous) formose catalyzed solution proton NMR.



Reaction Scheme S1. A Model for a Proto Metabolic Formose System on dry land.



Reaction Scheme S2. A Model for a Proto Metabolic Formose System at a hydrothermal vent.

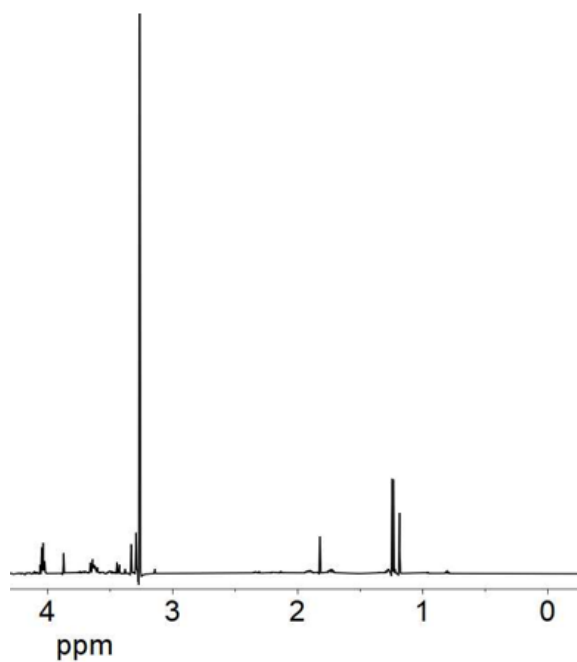


Figure S20. Sugar break down control. 0.167 Glucose solution heated at 90 C for 30 minutes at pH. 12.5 proton NMR. We see the same peaks for lactic acid as we do in our formose reactions.